P. Kaps, W. Nachbauer, and M. Mössner,
Determination of Kinetic Friction and Drag Area in Alpine Skiing,
Ski Trauma and Skiing Safety: 10th Volume, 1996

Reference: P. Kaps[1], W. Nachbauer[2], and M. Mössner[3], *Determination of Kinetic Friction and Drag Area in Alpine Skiing*, Ski Trauma and Skiing Safety: 10th Volume, ASTM STP 1266 (Philadelphia, US-PA) (C.D. Mote, R.J. Johnson, W. Hauser, and P.S. Schaff, eds.), American Society for Testing and Materials (ASTM), 1996, pp. 165–177.

Abstract: The coefficient of friction of skis on snow appears to be influenced by several factors, for example, speed, contact area, snow type and ski properties. The purpose of this study was to determine simultaneously the coefficient of kinetic friction and the drag area in straight running on a slope with varying inclination and in traversing on an inclined plane. Experimental measurements were taken using photo cells for straight running and by film analysis for traversing. The skier was modeled as a particle that moves on the surface of a slope. The equation of motion with the algebraic constraints of the track of the skier represents a differential-algebraic equation which was solved numerically. The coefficient of friction and the drag area were calculated by minimizing the sum of the square errors between computed and measured time data.

For straight running, the computed coefficient of friction and the drag area were in the same range as obtained by other methods. For traversing, the coefficient of friction could be determined but not the drag area. The skier traversed in an upright position at a speed from 0 to 17 m/s. In this range of velocity the drag area is not constant. It corresponds to critical Reynolds numbers where a sudden drop in the drag coefficient occurs if the body segments are approximated by cylinders.

The results indicate that in both cases the applied method is adequate for determining simultaneously the coefficient of kinetic friction and the drag area if these parameters are independent of the velocity.

[1]Inst. for Basic Sciences in Engineering, Univ. Innsbruck, AT. email: Peter.Kaps@uibk.ac.at
[2]Dept. of Sport Science, Univ. Innsbruck, AT
[3]Dept. of Sport Science, Univ. Innsbruck, AT

Nomenclature

A	projected area
A_c	contact area
α	slope inclination
β	traverse angle between fall line and direction of travel
C_d	drag coefficient
d	thickness of water film
D	diameter of a cylinder
η	coefficient of viscosity
F_c	friction force due to snow compaction, ploughing, etc.
F_d, F_f	drag and friction force
$\mathbf{F}_g$	gravitational force
$\mathbf{F}_a, \mathbf{F}_r$	vector of applied and reaction forces
k_1, k_n	air friction constant, see Eq 6, 7
l	height of a skater
L	characteristic length in Re
m	mass
μ	coefficient of friction
μ_1	velocity dependent part of coefficient of friction
N	normal force
ν	kinematic viscosity
Re	Reynolds number
ρ	density
s	arc length of path of skier
s_i	arc length at time t_i
t_i	measured time at ith photocell or for ith picture
θ_0	knee angle
θ_1	angle between trunk and horizontal line
v	velocity
V	characteristic velocity in Re
x_i, y_i	measured coordinates of skier at ith photocell

1 Introduction

When a ski glides over snow, the snow exerts forces on the ski. The ratio of the tangential force and the normal force is called the *coefficient of kinetic friction*. It is influenced by several factors, e.g. speed, contact area, loading, temperature, snow type (snow temperature, hardness, liquid-water content, texture) and ski properties (stiffness, thermal conductivity, base material, base roughness). The air resistance comprises all interactions between skier and air. The component parallel to the direction of motion is called *drag*, the normal component *lift*. The drag coefficient seems to be nearly constant for high velocities whereas it decreases for low velocities (Gorlin et al. [12]). In laboratory investigations, the coefficient of friction was commonly determined by means of friction meters consisting of rotational devices with built-in force transducers (e.g. Kuroiwa [19]). In skiing investigations, measurements were obtained in straight running using the towing method (e.g. Habel [13]) or the runout method (e.g. Habel [13], Leino and Spring [20]). The drag area is determined usually in wind channels (Gorlin et al. [12]). Erkkilä et al. [9] used roller-skis. The purpose of this study was to present a method to determine the coefficient of kinetic friction and the drag area simultaneously in straight running on a slope with varying inclination and in traversing on an inclined plane. The paper starts with a review on results for the kinetic friction and the drag area. The experimental work was performed in the surroundings of Seefeld, Austria. Then the equations of motion are formulated as differential-algebraic equations and results are presented for schussing in the fall line and for traversing.

2 Data collection

The straight running experiments were conducted on a 342 m long run with an altitude difference of 73 m (Fig 1). Nine photocells were installed about 25 cm above the snow surface and distributed along the run. The location of the photocells was determined by geodetic surveying using a theodolite. Time data of a skier gliding straight down the fall line in a tucked position were collected from all photocells (see Nachbauer et al. [26]).

In traversing, the path of the downhill ski boot was determined by film analysis. The length of the run was about 25 m, located on an 18° inclined plane (Fig 2). The traversing angle was about 40° to the horizontal. The sides of the traverse were marked by ropes equipped with black-painted tennis balls that defined a 1 m reference marker system. The skier was filmed with a 16 mm high-speed camera located laterally to the plane of motion of the skier. The width of the film field ranged from 4 to 6 m. The film speed was set at 100 frames per second. Ball-shaped markers were placed on the toepiece of the binding. The skier had to traverse in a straight line in an upright position. Side slipping was to be avoided. The coordinates of the marker were determined using the DLT method (Kaps et al. [18], Mössner et al. [24]). Barometric pressure and air temperature were measured in

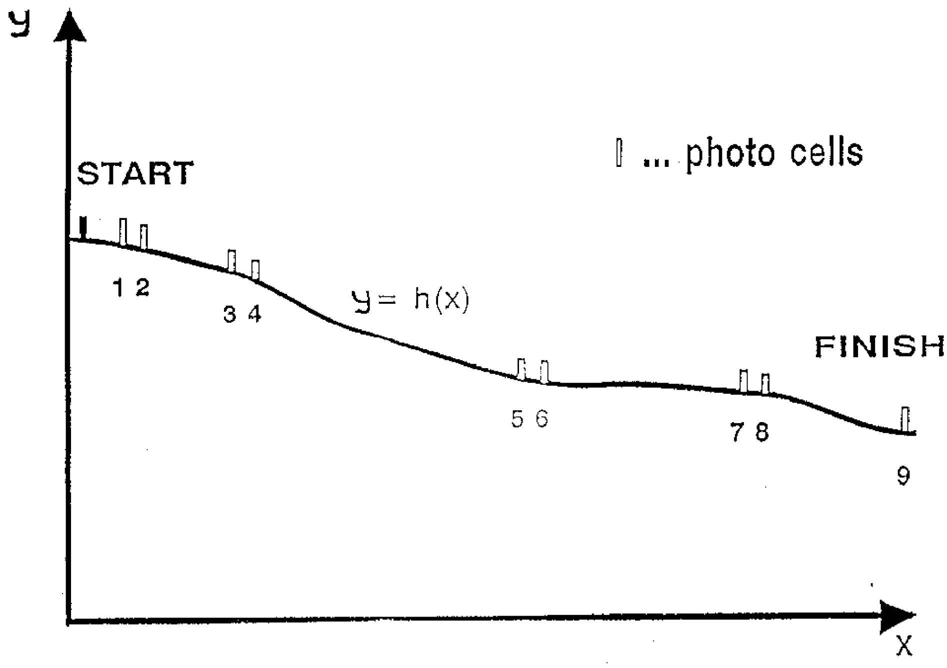

Fig. 1: Straight running experiments.

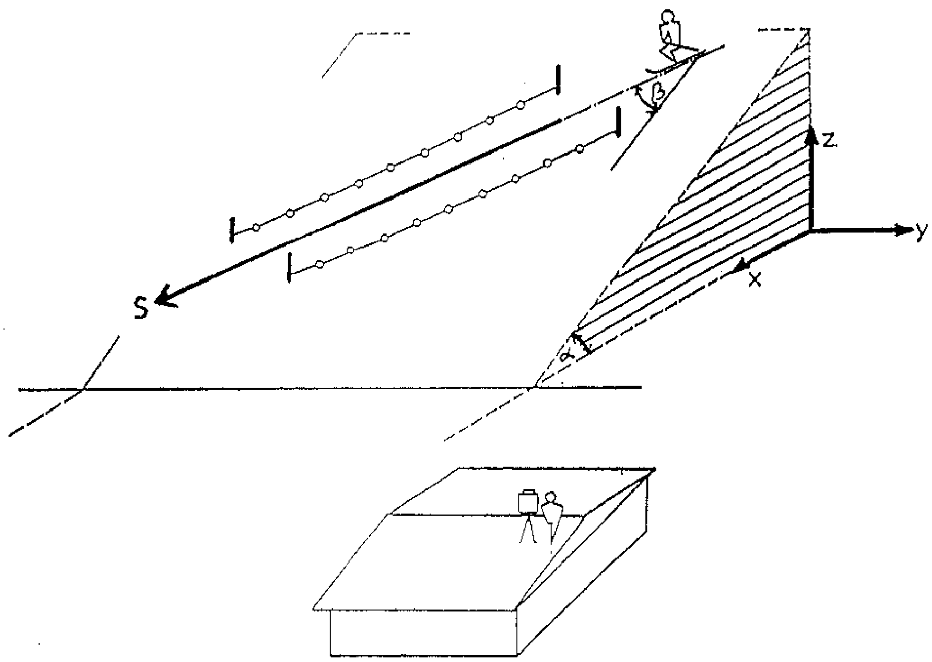

Fig. 2: Traversing experiments.

order to calculate the air density. The mass of the skier including his equipment was measured as well (see Haug [16]).

3 Kinetic friction

The friction between ski and snow is relatively small because the snow melts at the contact surface of the ski due to the heat produced by friction (Bowden and Hughes [5], Bowden [4]), but it is a complicated phenomenon which is understood only partly.. A thin water film covers at least part of the contact surface. Before we discuss kinetic friction more carefully, two facts from basic mechanics are stated.

1. Coulomb friction: If a rigid body is sliding on a rigid surface, there is a friction force F_f which is proportional to the normal force N by which the body is pressed onto the surface

$$F_f = \mu N, \tag{1}$$

where μ is the coefficient of kinetic friction. It is almost independent of the velocity.

2. Viscous friction: If two rigid bodies are moving on a liquid film of thickness d in between with a relative velocity v, the friction force is given by

$$F_f = \frac{\eta A_c v}{d}, \tag{2}$$

where A_c denotes the contact area and η the coefficient of viscosity.

For a review of the current research on the kinetic friction between ski and snow see Colbeck [6], Colbeck and Warren [8], Glenne [11], and Perla and Glenne [28]. The snow friction force can be separated into two components. One component is due to the ploughing, shearing, and compression action of a ski; this component is called F_c. The second component is the frictional interaction at the ski-snow interface, where three mechanisms dominate at different film thicknesses: dry, lubricated, and capillary friction. Dry friction occurs at low temperatures or low velocities when the water film is insufficient to prevent solid-to-solid interactions between ski and snow. For thick water films, there is a bridging between the slider and ice grains which are not carrying any load. This leads to an increase in friction (Colbeck [7]). Evans et al. [10], and Akkok et al. [2] presented careful investigations of *thermally controlled* kinetic friction of *ice*. However, they obtained results which suggest that the coefficient of kinetic friction μ is proportional to $1/v$, which is doubtful for our conditions in which higher velocities occur. For hard snow, F_c is usually disregarded. However, it seems that the influence of the ski stiffness on the ground pressure distribution is an important factor (Aichner [1]). The dry sliding friction can be described by a formula of type Eq 1. For the wet sliding friction, a formula of type Eq 2 should hold. Note that the thickness of the water film and the area of contact are not known. Ambach and Mayr [3] measured the thickness of the water film. We have the impression that the theoretical and empirical results are not consistent. Without doubt, μ depends on the velocity and the loading. As a guess, we modified Eq 1 by introducing a velocity dependent part

$$F_f = (\mu + \mu_1 v)N. \tag{3}$$

A partial result of the experimental results given later encourages such investigations. Note that a term proportional to v^2 cannot be separated from the air drag, at least for small changes of the load. Moreover, the dependence assumed in Eq 3 for the load is doubtful.

4 Drag area

The drag force F_d is given by

$$F_d = \frac{1}{2} C_d A \rho v^2, \tag{4}$$

where C_d denotes the drag coefficient, A the frontal projected area, ρ the density, and v the relative velocity between air and body. The drag coefficient C_d is usually assumed to be independent of the velocity. Habel [13], the Austrian pioneer in ski friction measurements, strongly stated that the drag coefficient for a skier does not depend on velocity as long as no aerodynamic means such as spoilers are used. Also, in Leino et al. [21] and Leino and Spring [20] a constant drag coefficient was used, but the traversing results given later could not be explained by this hypothesis. For the interpretation of these results we must recall some facts of aerodynamics (see Schlichting [30], Hoerner [17], and Schenau's excellent investigation of speed skating [32]). Especially for low velocities (up to 15 m/s) the drag coefficient depends on the velocity. Already 1972 Gorlin et al. [12] presented plots of the drag coefficients of skiers in different positions for the velocity range from 10 up to 45 m/s. The drag coefficient is roughly halved from its initial value at a velocity of 10 m/s to a "nearlyconstant value for velocities between 15 and 45 m/s.

In fluid dynamics the Reynolds number Re plays an essential role. We ask, under what conditions do geometrically similar bodies produce a similar picture of streamlines. The answer is that at similar points the ratio of the forces must be the same, independent of time. We consider a stationary flow which streams with a velocity u mainly in direction x. If one assumes inertial forces $\rho u \frac{\partial u}{\partial x}$ and friction forces $\eta \frac{\partial^2 u}{\partial y^2}$ only, the ratio of these forces is a dimensionless number which is called the Reynolds number:

$$\frac{\rho u \partial u/\partial x}{\eta \partial^2 u/\partial y^2} = \frac{\rho V^2/L}{\eta V/L^2} = \frac{\rho V L}{\eta} = \frac{VL}{\nu} =: Re \tag{5}$$

where V is a characteristic velocity and L a characteristic length. $\nu = \eta/\rho$ is called kinematic viscosity. Thus, the flow around two similar bodies is similar in all situations, for which Reynolds numbers are equal (see e.g. Schlichting [30]). In air, the flows around cylinders with diameters 1 and 2 are similar when the unperturbed velocities are 10 and 5, respectively.

The drag force has two components, the *friction* drag and the *pressure* drag. Friction drag is determined by friction forces in the boundary layer. When friction drag dominates, C_d is inversely proportional to the velocity v (Stokes' law) and F_d is proportional to v. This situation occurs for $Re \leq 1$. When Re increases from $Re = 1$ to $Re = 10^3$, the air behind a body becomes turbulent. The velocity in front of the body is almost zero and increases behind the place where the boundary layer is separated from the surface. This high velocity v leads to a low pressure behind the body. In front of the body the pressure is about $\frac{1}{2}\rho v^2$ higher than behind the body. The pressure drag force is nearly proportional to $\frac{1}{2}A\rho v^2$. The drag coefficient contains the other influences such as shape or nature of the surface (clothing). For regular bodies such as spheres or cylinders (including elliptical cross sections) the dependence of C_d as a function of Re is known. Wind tunnel experiments show that C_d is nearly constant for Reynolds numbers in the range $10^3 < Re < 10^5$. This is due to the fact that the boundary layer separates from the surface at the same location. In the range $10^5 < Re < 10^6$, C_d rapidly decreases to a lower level. Due to turbulence in the boundary layer itself, the place of separation of the boundary layer from the surface shifts to a more downstream position resulting in a smaller wake behind the body. The kinematic viscosity ν of air is given by $\nu = 1.4 \times 10^{-5}\ m^2/s$. If one puts the diameter of the trunk $D = 0.4\ m$ or the thighs $D = 0.2\ m$ as characteristic length, one obtains from a critical Reynolds number 2.8×10^5 critical velocities of $V = 9.8\ m/s$ and $V = 19.6\ m/s$, respectively. Already Gorlin et al. [12] point out that the value of C_d for different positions may be individually strongly different. An optimal position must be choosen for each skier separately. Changes in the position which are in the first view not essential might affect the value of C_d by 10 to 20%. Even during the test, elite skiers were not able to remain completely in an optimal position.

Schenau [32] investigated skaters with a knee angle θ_0 and an angle θ_1 between the trunk and a horizontal line. The air friction constant k_1 at a velocity $v = 12\ m/s$

$$k_1 = \frac{1}{2}C_d A\rho \tag{6}$$

depends obviously on θ_0 and θ_1. The value of k_1 at a reference position of $\theta_1 = 15°$ and $\theta_0 = 110°$ is denoted by k_n. Schenau [32] found the relation

$$k_1 = k_n(0.798 + 0.013\theta_1) \times (0.167 + 0.00757\theta_0) \tag{7}$$

for values near to the reference position. Although C_d depends strongly on the individual skater, Schenau [32] found the following relationship between k_n, the height l, and the mass m of a skater:

$$k_n = 0.0205\ l^3\ m. \tag{8}$$

In Nachbauer and Kaps [25], the drag area of skiers in a tucked position was considered as a function of the mass only. With the help of Eq 8, Schenau [32] could predict the drag force of six skaters within a standard deviation of 2%. For the dependence of k_1 on the velocity, Schenau [32] found

$$\frac{k_1(v)}{k_n} = \begin{cases} 4.028 - 0.809 \ln v - 0.189v + 0.00866v^2 & \text{for } 7 < v < 14 \text{ m/s}, \\ 1.561 - 0.0705v + 0.00188v^2 & \text{for } 14 < v < 19 \text{ m/s}. \end{cases} \tag{9}$$

The correlations of the first and second expression within the brace are given by $r = 0.99$ and $r = 0.81$, respectively.

Erkkilä et al. [9] measured the drag of a skier with roller-skis. The drag area was found to decrease linearly with velocity increase in the velocity range 5.5 to 10 m/s. The slope was 0.043 for a skier in a semi-squatting position. Spring et al. [31] measured the drag area of cross country skiers gliding on roller-skis. In the velocity range from 5.5 to 10.5 m/s the drag area was nearly constant. For a skier in a racing suit the drag area was $0.65 \pm 0.05\ m^2$ in an upright posture, and $0.27 \pm 0.03\ m^2$ in a semi-squatting posture.

Roberts [29] used a model in which he approximated the trunk, the lower legs and the upper arms as cylinders. Depending on the Reynolds number he used the following values for the drag coefficient:

$$C_d = \begin{cases} 1.2 & \text{for } 6 \times 10^3 < Re < 2 \times 10^5, \\ 1.0 & \text{for } 2 \times 10^5 < Re < 4 \times 10^5, \\ 0.3 & \text{for } Re > 4 \times 10^5. \end{cases} \tag{10}$$

5 Equations of motion

The equations of motion are formulated as a system of differential-algebraic equations (DAEs):

$$\begin{aligned} \mathbf{M}\ddot{\mathbf{x}} &= \mathbf{F}_a + \mathbf{F}_r \\ \mathbf{g}(\mathbf{x}) &= \mathbf{0}. \end{aligned} \tag{11}$$

The first expression is a system of n_x second order differential equations for the n_x unknown components of $\mathbf{x}$. $\mathbf{M}$ denotes the mass matrix, $\mathbf{F}_a$ the applied forces, and $\mathbf{F}_r$ the constraint or reaction forces. $\mathbf{g}(\mathbf{x}) = \mathbf{0}$ is a system of n_g algebraic equations which are called *position* constraint equations. From d'Alembert's principle it follows for the reaction forces

$$\mathbf{F}_r = -\mathbf{G}^T \boldsymbol{\lambda}. \tag{12}$$

$\mathbf{G}^T$ denotes the transpose of the Jacobian matrix

$$\mathbf{G} = \frac{\partial \mathbf{g}(\mathbf{x})}{\partial \mathbf{x}} = \mathbf{g}_{\mathbf{x}}. \tag{13}$$

The vector $\boldsymbol{\lambda}$ is called the Lagrange multiplier. Its components are additional unknowns. Equation 11 represents a system of DAEs with *index* 3 since it is necessary to differentiate Eq 11 three times to obtain a system of ordinary differential equations in the variables $(\mathbf{x}, \boldsymbol{\lambda})$. If the position constraints in Eq 11 are differentiated with respect to time, one obtains the *velocity* constraints

$$\mathbf{g}_{\mathbf{x}}\dot{\mathbf{x}} = \mathbf{0}. \tag{14}$$

Replacement of the position constraints in Eq 11 by the velocity constraints yields a system of DAEs of index 2. This can be solved by recently developed codes, for example, MEXX21 (Lubich [22], Lubich et al. [23]). The reaction forces $\mathbf{F}_r$ are computed automatically and need not be provided by the user of such a code.

The skier is modeled as a mass point with coordinates $\mathbf{x} = (x, y)$ or $\mathbf{x} = (x, y, z)$ in the two-dimensional or three-dimensional case, respectively. The dimension n_x of $\mathbf{x}$ is given by 2 or 3, correspondingly. With help of the constraints $\mathbf{g}(\mathbf{x}) = \mathbf{0}$ an arbitrary path can be defined, for example in two dimensions by

$$y = h(x) \tag{15}$$

or in three dimensions by

$$z = h(x, y), \quad y = y(x). \tag{16}$$

Thus n_g the dimension of $\mathbf{g}$ is given by 1 or 2. If the applied forces $\mathbf{F}_a$ are known, the motion $\mathbf{x}(t)$ of a skier can be computed as a function of time t. We have used an earlier version of the code MEXX21. More detailed information on DAEs is given in Hairer and Wanner [15], and representation of the equations of motion as DAEs in Haug [16]. The applied forces consist of the gravitational force $\mathbf{F}_g$, the drag force $\mathbf{F}_d$ and the friction force $\mathbf{F}_f$

$$\mathbf{F}_a = \mathbf{F}_g + \mathbf{F}_d + \mathbf{F}_f. \tag{17}$$

5.1 Straight running

The path of the skier is given by Eq 15, the slope by

$$\tan\alpha = h'(x) \tag{18}$$

(see Fig 3). Note in the situation of Fig 3, it holds that $\alpha < 0$.

For the unit vectors $\mathbf{t}$ and $\mathbf{n}$ in the tangential and normal directions, respectively, and the reaction force $\mathbf{F}_r$ in Eq 11 it holds that

$$\mathbf{t} = \begin{pmatrix} \cos\alpha \\ \sin\alpha \end{pmatrix}, \quad \mathbf{n} = \begin{pmatrix} -\sin\alpha \\ \cos\alpha \end{pmatrix}, \quad \mathbf{F}_r = -\begin{pmatrix} -\tan\alpha \\ 1 \end{pmatrix}\lambda = N\,\mathbf{n} \text{ with } N = -\frac{\lambda}{\cos\alpha}. \tag{19}$$

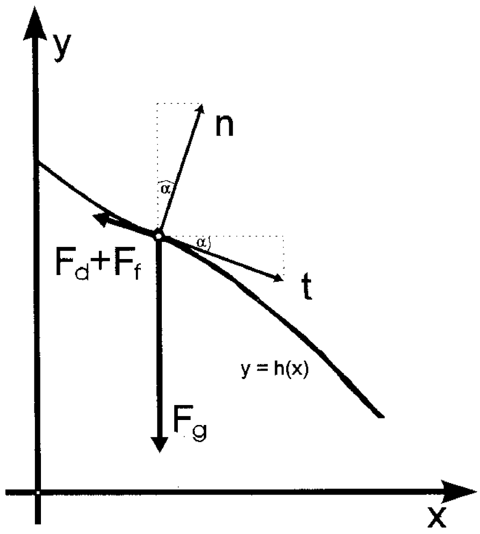

Fig. 3: Model of skier.

The normal force N depends on the Lagrange multiplier λ. If one considers the kinetic friction Eq 1 and the drag Eq 4, one obtains

$$\mathbf{F}_f + \mathbf{F}_d = -(\frac{1}{2}\rho(\dot{x}^2 + \dot{y}^2)C_d A + \mu N)\mathbf{t}. \tag{20}$$

The equation of motion is given by:

$$m\begin{pmatrix}\ddot{x}\\ \ddot{y}\end{pmatrix} = \begin{pmatrix}0\\ -mg\end{pmatrix} + \mathbf{F}_f + \mathbf{F}_d + \mathbf{F}_r, \quad y - h(x) = 0. \tag{21}$$

The applied force depends on the Lagrange multiplier λ. If λ becomes positive, the skier will be in the air and the constraint equation is no longer valid.

5.2 Traversing

For traversing on an inclined plane (Fig 2) α and β are constant. By introducing the arc length s as the dependent variable, one obtains for the equation of motion the well known ordinary differential equation (see Kaps et al. [18]):

$$\begin{aligned}\ddot{s} &= a + b\dot{s}^2\\ a &= -g\sin\alpha\cos\beta - \mu g\cos\alpha\\ b &= -\frac{1}{2m}\rho A C_d.\end{aligned} \tag{22}$$

The initial conditions are given by

$$s(0) = s_0, \qquad \dot{s}(0) = v_0. \tag{23}$$

Usually we choose $s_0 = 0$. We tried to vary the initial velocity v_0 to obtain different mean velocities in the test runs (slow, moderate, fast). To this aim, the skier started from different heights. Therefore, the initial velocity is treated as an unknown parameter. Writing Eq 22 as a first order system, the new variables s and $w = \dot{s} - v_0$ are introduced. This yields to

$$\begin{aligned} \dot{s} &= w + v_0 \\ \dot{w} &= -\frac{\rho}{2m} C_d A (w + v_0)^2 - \mu g \cos\alpha - g \sin\alpha \cos\beta \\ s(0) &= 0, \qquad w(0) = 0. \end{aligned} \tag{24}$$

The drag area and the coefficient of friction must remain nonnegative. Thus, these expressions are written as squares of the corresponding parameters

$$p_1^2 = C_d A, \qquad p_2^2 = \mu, \qquad \text{and} \qquad p_3 = v_0. \tag{25}$$

To obtain a least-squares solution, one needs the derivatives of the components of Eq 24 with respect to the parameters. A numerical differentiation is not satisfactory since the numerical code would usually stop before reaching the minimum. With the following abbreviations

$$\begin{aligned} y_1 &= s, & y_3 &= \frac{\partial s}{\partial p_1}, & y_5 &= \frac{\partial s}{\partial p_2}, & y_7 &= \frac{\partial s}{\partial p_3}, \\ y_2 &= w, & y_4 &= \frac{\partial w}{\partial p_1}, & y_6 &= \frac{\partial w}{\partial p_2}, & y_8 &= \frac{\partial w}{\partial p_3} \end{aligned} \tag{26}$$

one obtains the so-called *variational equations* (see, e.g., Hairer et al. [14]):

$$\begin{aligned} \dot{y}_1 &= y_2 + p_3 \\ \dot{y}_2 &= -\frac{\rho}{2m}(y_2 + p_3)^2 p_1^2 - g \cos\alpha\, p_2^2 - g \sin\alpha \cos\beta \\ \dot{y}_3 &= y_4 \\ \dot{y}_4 &= -\frac{\rho}{m}(y_2 + p_3) y_4 p_1^2 - \frac{\rho}{m}(y_2 + p_3)^2 p_1 \\ \dot{y}_5 &= y_6 \\ \dot{y}_6 &= -\frac{\rho}{m}(y_2 + p_3) y_6 p_1^2 - 2g \cos\alpha\, p_2 \\ \dot{y}_7 &= y_8 + 1 \\ \dot{y}_8 &= -\frac{\rho}{m}(y_2 + p_3)(y_8 + 1) p_1^2 \end{aligned} \tag{27}$$

with the initial values

$$y_i(0) = 0, \qquad i = 1, \ldots, 8. \tag{28}$$

This system of ordinary differential equations is integrated numerically.

6 Experimental results

6.1 Straight running

According to the experimental setup given earlier we have measured the time t_i and the coordinates x_i, y_i when the skier passed the ith photo cell. The solution of the equation of motion (Eq 21) depends on the parameter $\mathbf{p} = (\sqrt{C_d A}, \sqrt{\mu}, v_0)$. We have computed the times $t(x_i, \mathbf{p})$ at which the x-component of the solution was equal to x_i. Note that a root finding algorithm is necessary. The parameters were computed by minimizing the sum of error squares

$$\Sigma(\mathbf{p}) = \sum_{i=1}^{9} (t(x_i, \mathbf{p}) - t_i)^2. \tag{29}$$

We used the program E04FCF of the NAG library [27]. This program is based on the Gauss-Newton method near to the solution. It computes the derivatives with respect to the parameters numerically. We include an additional computation where the kinetic friction in Eq 19 was replaced by Eq 3. In Tab 1, results of a fast run are presented. In addition to the deviations Σ, the gradient g of Σ is given. At a minimum it holds $g = 0$. $g^T g$ is the square of the Euclidean length of g.

v_0	$C_d A$	μ	μ_1	Σ	$g^T g$
3.4	0.22	$8.5 \cdot 10^{-3}$	0	0.11	0.11
3.1	0.22	$8.1 \cdot 10^{-3}$	$8.3 \cdot 10^{-5}$	0.18	0.47

Tab. 1: Results for straight running.

The results show that it has been difficult to obtain the real minimum, since the value of $g^T g$ is relatively high. The computed coefficient of friction was 0.0085, which is below the range obtained by the towing and runout method. By these methods values between 0.01 and 0.25 were obtained. The drag area was 0.22 m^2. This is in agreement with unpublished wind tunnel experiments of the Austrian Ski Federation, in which the drag area of male world class racers was between 0.13 and 0.19 m^2. The results for a velocity dependent kinetic friction gave errors which are only slightly higher.

6.2 Traversing

According to the experimental setup of Fig 2, we have measured the position of a point at the ski binding s_i at time t_i corresponding to the ith picture. For the computation of the minimum, we used the algorithm E04GDF of the NAG library [27], which needs the derivatives of s and $\dot{s}$ with respect to the parameters. Therefore, we solved the equation of motion (Eq 27) in variational form. The parameters $\mathbf{p}$

μ	$\Delta\mu$	$v_0(m/s)$	$v_f(m/s)$
0.064	0.060 – 0.067	0.6	10.6
0.128	0.108 – 0.150	11.0	13.4
0.153	0.136 – 0.171	14.7	16.6

Tab. 2: Results for traversing: Coefficients of friction (μ) with 90% confidence intervals ($\Delta\mu$), initial (v_0) and final velocities (v_f).

were computed by minimizing the sum of error squares

$$\Sigma(\mathbf{p}) = \sum_{i=1}^{m} (s(t_i, \mathbf{p}) - s_i)^2. \tag{30}$$

In Tab 2 the traversing results for different velocities are summarized. The computed coefficients of friction were between 0.06 and 0.15. Note that the normal force N in the equation of motion was given by $N = mg\cos\alpha$. We ignored the fact that the skier is actually gliding on a small band which is cut out of the inclined plane. The values of the friction coefficients are relatively high compared with those of straight running. A reason might be that compression, ploughing, and shearing forces contribute to a larger μ. The increase of μ with increasing velocity is not necessarily a velocity effect, as the snow conditions varied considerably throughout the measurements due to increasing solar radiation. The increase in the length of the confidence interval $\Delta\mu$ for increasing velocities is not caused by a decreasing number of data points for low, medium, and high velocity, as one might expect. We used in all cases approximately 100 data points. For low velocities, only every third picture was used. For the drag area the value 0 was obtained. The confidence interval was infinitely large.

In the earlier „drag area“section, arguments (Gorlin et al. [12], Schenau [32], Roberts [29]) were given that the drag area depends on the velocity in the investigated range of velocities. This leads us to the assumption that the model (Eq 4) is not correct for traversing. Note that during straight running the skier used a tucked position, whereas during traversing he used an upright position. We have also performed an experiment in which the skier was loaded in order to investigate the dependence of the kinetic friction on the load. The mass of the skier was 88 kg, the load 69 kg. One obtained $\mu = 0.049$ and $C_dA = 0.89$. The 90% confidence intervals were $\Delta\mu = [0.049, 0.053]$ and $\Delta(C_dA) = [0.61, 1.12]$, and the velocities were $v_0 = 0.37\ m/s$ and $v_f = 10.5\ m/s$. Thus the drag area could be computed within a still acceptable interval of confidence. An explanation could be that in the case of a skier loaded with a lead vest and a knapsack, the critical Reynolds number was reached at a lower velocity.

7 Conclusion

In this study a new method to determine the coefficient of kinetic friction μ and the drag area C_dA was presented. For straight running μ and C_dA were computed simultaneously for a track with variable inclination. The results correspond well with literature values. To our knowledge, we have performed the first measurements for traversing. We could determine the kinetic friction. Values of 0.06 to 0.15 appear to be high compared with those for straight running. However, due to increasing solar radiation the snow became wet and soft - a situation in which the friction is usually high. The drag area could not be determined. This failure is probably due to inappropriate model assumptions. The skier traversed in an upright position at speeds from 0 to 17 m/s. In this velocity range the drag area is probably not constant as it was assumed in the calculations.

The method requires the collection of position/time data of the skier. Two measurement techniques were tested: timing and cinematography. In the first case, accurate time (± 0.1 ms) and position data (± 1 cm) of nine photocells were obtained at a long test run of about 340 m. In the second case the time data are assumed to be exact and the position data have an error of ± 10 cm. This relatively large error is mainly caused mainly by two facts: first, the test course was not ideally planar; and second, the track of the skier was approximated by a straight line. This task could not be performed by the skier exactly. The results indicate that both methods are adequate for collecting the required data. However, the analysis of the cinematographical data is much more complicated and time consuming.

For more detailed investigations regarding the dependence of the drag area on velocity and the dependence of kinetic friction on velocity or loading, one has to improve the measurement setup. This was accomplished on the runout at the Olympic ski jumping site in Seefeld, where 20 photocells were built up and geodetically surveyed. Time data of straight runs of a skier were collected but have not yet been analyzed. At the same time, video measurements were taken which will allow to compare the two data collection methods.

Acknowledgment

This study was supported in part by a grant of the Austrian Research Foundation and the Austrian Ski Federation.

References

[1] N. Aichner, *Bodendruckverteilung und Formänderungswiderstand beim gleitenden Schi*, Ph.D. Thesis, Graz University of Technology, AT, 1978.

[2] M. Akkok and C.M. Ettles and, *Parameters Affecting the Kinetic Friction of Snow*, Journal of Tribology **109** (1987), 552–561.

[3] W. Ambach and, *Ski Gliding and Water Film*, Cold Regions Science and Technology **5** (1981), 59–65.

[4] F.P. Bowden, *Friction on Snow and Ice*, Proceedings of the Royal Society of London **A217** (1953), 462–478.

[5] F.P. Bowden and T.P. Hughes, *The Mechanism of Sliding on Ice and Snow*, Proceedings of the Royal Society of London **A172** (1939), 280–298.

[6] S.C. Colbeck, *A Review of the Processes that Control Snow Friction*, Technical Report 92-2, Cold Regions Research and Engineering Laboratory (CRREL), Hanover, US-NH, 1992.

[7] S.C. Colbeck, *The Kinetic Friction of Snow*, Journal of Glaciology **34** (1988), 78–86.

[8] S.C. Colbeck and G.C. Warren, *The Thermal Response of Downhill Skis*, Journal of Glaciology **37** (1991), 228–235.

[9] J. Erkkilä, T. Hämäläinen, P. Pihkala, S. Savolainen, and E. Spring, *A Cinematographic Method for Determination of the Kinetic Friction of Skis on Snow*, Report Series in Geophysics, vol. 21, University of Helsinki, FI, 1985.

[10] C.D.B. Evans, J.F. Nye, and K.J. Cheeseman, *The Kinetic Friction of Ice*, Proceedings of the Royal Society of London **A347** (1976), 493–512.

[11] B. Glenne, *Sliding Friction and Boundary Lubrication of Snow*, Journal of Tribology **109** (1987), 614–617.

[12] S.M. Gorlin, M.M. Maseev, W.A. Zyrjanow, and L.L. Remizov, *Sliding Friction and Boundary Lubrication of Snow*, Teorija i praktika fizicheskoj kultury **2** (1972), 65–66.

[13] B. Habel, *Über die Bestimmung von Luftwiderstand und Gleitreibung beim Skilauf*, Europa-Sport **20** (1968), 950–955.

[14] E. Hairer, S.P. Nørsett, and G. Wanner, *Solving Ordinary Differential Equations I. Nonstiff Problems*, 2nd ed., Springer Series in Computational Mathematics, vol. 8, Springer, Berlin, DE, 1993.

[15] E. Hairer and G. Wanner, *Solving Ordinary Differential Equations II. Stiff and Differential-Algebraic Problems*, Springer Series in Computational Mathematics, vol. 14, Springer, Berlin, DE, 1991.

[16] E.J. Haug, *Computer Aided Kinematics and Dynamics of Mechanical Systems. Vol. I: Basic Methods*, Allyn and Bacon, Boston, US-MA, 1989.

[17] S.F. Hoerner, *Fluid-Dynamic Drag, Practical Information on Aerodynamic Drag and Hydrodynamic Resistance*, published by the author, New York, US-NY, 1965.

[18] P. Kaps, M. Mössner, and W. Nachbauer, *Messung von Gleitreibung und Luftwiderstand bei Hangschrägfahrt*, Report, Institute for Basic Sciences in Engineering, University of Innsbruck, AT, May 1992.

[19] D. Kuroiwa, *The Kinetic Friction on Snow and Ice*, Journal of Glaciology **19** (1977), 141–152.

[20] M.A.H. Leino and E. Spring, *Determination of the Coefficient of Kinetic Friction between Ski and Snow from Gliding Velocity of a Skier*, Report Series in Geophysics, vol. 19, University of Helsinki, FI, 1984.

[21] M.A.H. Leino, E. Spring, and H. Suominen, *Methods for the Simultaneous Determination of Air Resistance to a Skier and the Coefficient of Friction of his Skis on the Snow*, Wear **86** (1983), 101–104.

[22] C. Lubich, *Extrapolation Integrators for Constrained Multibody Systems*, Impact of Computing in Science and Engineering **3** (1991), 213–234.

[23] C. Lubich, U. Nowak, U. Pöhle, and C. Engstler, *MEXX – Numerical Software for the Integration of Constrained Mechanical Multibody Systems*, Preprint SC 92-12, Konrad-Zuse-Zentrum für Informationstechnik (ZIB), Berlin, DE, 1992.
`http://www.zib.de/Numerik/numsoft/CodeLib/index.en.html`

[24] M. Mössner, P. Kaps, and W. Nachbauer, *A Method for Obtaining 3-D Data in Alpine Skiing Using Pan and Tilt Cameras with Zoom Lenses*, Skiing Trauma and Safety, 10th vol., ASTM STP 1266 (Philadelphia, US-PA) (C.D. Mote, R.J. Johnson, W. Hauser, and P.S. Schaff, eds.), American Society for Testing and Materials (ASTM), 1996, pp. 155–164.

[25] W. Nachbauer and P. Kaps, *Fahrzeitbestimmende Faktoren beim Schussfahren*, Biomechanik der Sportarten. Band 2: Biomechanik des alpinen Skilaufs (F. Fetz and E. Müller, eds.), Ferdinand Enke Verlag, Stuttgart, DE, 1991, pp. 101–111.

[26] W. Nachbauer, P. Schröcksnadl, and B. Lackinger, *Effects of Snow and Air Conditions on Ski Friction*, Skiing Trauma and Safety, 10th vol., ASTM STP 1266 (Philadelphia, US-PA) (C.D. Mote, R.J. Johnson, W. Hauser, and P.S. Schaff, eds.), American Society for Testing and Materials (ASTM), 1996, pp. 178–185.

[27] Numerical Algorithms Group, NAG Ltd., Oxford, GB.
email: `sales@nag.co.uk www`. URL: `http://www.nag.co.uk/`.

[28] R.I. Perla and B. Glenne, *Skiing*, Handbook of snow (D.M. Grey and D.H. Male, eds.), Pergamon Press, Toronto, CA, 1981, pp. 709–740.

[29] C.C. Roberts, *Numerical Modeling of the Transient Dynamics of a Skier while Gliding*, Biomechanics in Sport – A (E.D. Rekow et al., ed.), The American Society of Mechanical Engineers, New York, US-NY, 1987, pp. 77–82.

[30] H. Schlichting, *Grenzschichttheorie*, Verlag G. Braun, Karlsruhe, DE, 1958.

[31] E. Spring, S. Savolainen, J. Erkkilä, T. Hämäläinen, and P. Pihkala, *Drag Area of a Cross-Country Skier*, International Journal of Sport Biomechanics **4** (1988), 103–113.

[32] G.J. van Ingen Schenau, *The Influence of Air Friction in Speed Skating*, Journal of Biomechanics **15** (1982), 449–458.